



Constraining the magnitude of the Chiral Magnetic Effect with Event Shape Engineering in Pb–Pb collisions at $\sqrt{s_{\text{NN}}} = 2.76$ TeV

ALICE Collaboration*

ARTICLE INFO

Article history:

Received 27 September 2017

Received in revised form 21 November 2017

Accepted 8 December 2017

Available online 12 December 2017

Editor: L. Rolandi

ABSTRACT

In ultrarelativistic heavy-ion collisions, the event-by-event variation of the elliptic flow v_2 reflects fluctuations in the shape of the initial state of the system. This allows to select events with the same centrality but different initial geometry. This selection technique, Event Shape Engineering, has been used in the analysis of charge-dependent two- and three-particle correlations in Pb–Pb collisions at $\sqrt{s_{\text{NN}}} = 2.76$ TeV. The two-particle correlator $\langle \cos(\varphi_\alpha - \varphi_\beta) \rangle$, calculated for different combinations of charges α and β , is almost independent of v_2 (for a given centrality), while the three-particle correlator $\langle \cos(\varphi_\alpha + \varphi_\beta - 2\Psi_2) \rangle$ scales almost linearly both with the event v_2 and charged-particle pseudorapidity density. The charge dependence of the three-particle correlator is often interpreted as evidence for the Chiral Magnetic Effect (CME), a parity violating effect of the strong interaction. However, its measured dependence on v_2 points to a large non-CME contribution to the correlator. Comparing the results with Monte Carlo calculations including a magnetic field due to the spectators, the upper limit of the CME signal contribution to the three-particle correlator in the 10–50% centrality interval is found to be 26–33% at 95% confidence level.

© 2017 The Author(s). Published by Elsevier B.V. This is an open access article under the CC BY license (<http://creativecommons.org/licenses/by/4.0/>). Funded by SCOAP³.

Parity symmetry is conserved in electromagnetism and is maximally violated in weak interactions. In strong interactions, global parity violation is not observed even though it is allowed by quantum chromodynamics. Local parity violation in strong interactions might occur in microscopic domains under conditions of finite temperature [1–4] due to the existence of the topologically non-trivial configurations of the gluonic field, instantons and sphalerons. The interactions between quarks and gluonic fields with non-zero topological charge [5] change the quark chirality. A local imbalance of chirality, coupled with the strong magnetic field produced in heavy-ion collisions ($B \sim 10^{15}$ T) [6–8], would lead to charge separation along the direction of the magnetic field, which is on average perpendicular to the reaction plane (the plane of symmetry defined by the impact parameter vector and the beam direction), a phenomenon called Chiral Magnetic Effect (CME) [9–12]. Since the sign of the topological charge is equally probable to be positive or negative, the charge separation averaged over many events is zero. This makes the observation of the CME experimentally difficult and possible only via correlation techniques.

Azimuthal anisotropies in particle production relative to the reaction plane, often referred to as anisotropic flow, are an important observable to study the system created in heavy-ion collisions [13, 14]. Anisotropic flow arises from the asymmetry in the initial geometry of the collision. Its magnitude is quantified via the coefficients v_n in a Fourier decomposition of the charged particle azimuthal distribution [15,16]. Local parity violation would result in an additional sine term [17]

$$\frac{dN}{d\Delta\varphi_\alpha} \sim 1 + 2v_{1,\alpha} \cos(\Delta\varphi_\alpha) + 2a_{1,\alpha} \sin(\Delta\varphi_\alpha) + 2v_{2,\alpha} \cos(2\Delta\varphi_\alpha) + \dots \quad (1)$$

where $\Delta\varphi_\alpha = \varphi_\alpha - \Psi_{\text{RP}}$, φ_α is the azimuthal angle of the particle of charge α (+, –) and Ψ_{RP} is the reaction-plane angle. The first ($v_{1,\alpha}$) and the second ($v_{2,\alpha}$) coefficients are called directed and elliptic flow, respectively. The $a_{1,\alpha}$ coefficient quantifies the effects from local parity violation. Since the average $\langle a_{1,\alpha} \rangle = 0$ over many events, one can only measure $\langle a_{1,\alpha}^2 \rangle$ or $\langle a_{1,+} a_{1,-} \rangle$. The charge-dependent two-particle correlator

$$\delta_{\alpha\beta} \equiv \langle \cos(\varphi_\alpha - \varphi_\beta) \rangle = \langle \cos(\Delta\varphi_\alpha) \cos(\Delta\varphi_\beta) \rangle + \langle \sin(\Delta\varphi_\alpha) \sin(\Delta\varphi_\beta) \rangle \quad (2)$$

* E-mail address: alice-publications@cern.ch.

is not convenient for such a study, because along with the signal $\langle a_{1,\alpha} a_{1,\beta} \rangle$ (β denotes the charge) there is a much stronger contribution from correlations unrelated to the azimuthal asymmetry in the initial geometry (“non-flow”). These correlations largely come from the inter-jet correlations and resonance decays. To increase the CME contribution it was proposed to use the following correlator [17]

$$\begin{aligned} \gamma_{\alpha\beta} &\equiv \langle \cos(\varphi_\alpha + \varphi_\beta - 2\Psi_{RP}) \rangle \\ &= \langle \cos(\Delta\varphi_\alpha) \cos(\Delta\varphi_\beta) \rangle - \langle \sin(\Delta\varphi_\alpha) \sin(\Delta\varphi_\beta) \rangle \end{aligned} \quad (3)$$

that measures the difference between the correlation projected onto the reaction plane and perpendicular to it. In practice, the reaction-plane angle is estimated by constructing the event plane angle Ψ_2 using azimuthal particle distributions, which is why this correlator is often described as a three-particle correlator. This correlator suppresses background contributions at the level of v_2 , the difference between the particle production in-plane and out-of-plane. Examples of such background sources are the local charge conservation (LCC) coupled with elliptic flow [18,19], momentum conservation [19–21], and directed-flow fluctuations [22]. The most significant background source for CME measurements is the LCC.

The measurements of charge-dependent azimuthal correlations performed at the Relativistic Heavy Ion Collider (RHIC) [23–26] and the Large Hadron Collider (LHC) [27,28] are in qualitative agreement with the expectations for the CME. However, the interpretation of these experimental results is complicated due to possible background contributions. The Event Shape Engineering (ESE) technique was proposed to disentangle background contributions from the potential CME signal [29]. This method makes it possible to select events with eccentricity values significantly larger or smaller than the average in a given centrality class [30,31] since v_2 scales approximately linearly with eccentricity [32]. Centrality estimates the degree of overlap between the two colliding nuclei, with low percentage values corresponding to head-on collisions. The CME contribution is expected to mainly scale with the magnetic field strength and to not have a strong dependence on the eccentricity [33], while the background varies significantly. Therefore ESE provides a unique tool to separate the CME signal from the background for the three-particle correlator.

The CMS Collaboration has recently reported the measurement of the three-particle correlator $\gamma_{\alpha\beta}$ in p–Pb collisions at $\sqrt{s_{NN}} = 5.02$ TeV [34], where the direction of the magnetic field is expected to be uncorrelated to the reaction plane [35]. The magnitude of the correlator in p–Pb and Pb–Pb collisions is comparable for similar final-state charged-particle multiplicities. This measurement indicates that the contribution of the CME to this observable in this multiplicity range is small.

In this paper we report the measurements of the two-particle correlator $\delta_{\alpha\beta}$, the three-particle correlator $\gamma_{\alpha\beta}$, and the elliptic flow v_2 of unidentified charged particles. These measurements are performed for shape selected and unbiased events in Pb–Pb collisions at $\sqrt{s_{NN}} = 2.76$ TeV. An upper limit on the CME contribution is deduced from comparisons of the observed dependence of the correlations on the event v_2 to that estimated using Monte Carlo (MC) simulations of the magnetic field of spectators with different initial conditions. While this paper was in preparation, a paper employing a similar approach to estimate the fraction of the CME signal in the three-particle correlator was submitted by the CMS Collaboration [36].

The data sample recorded by ALICE during the 2010 LHC Pb–Pb run at $\sqrt{s_{NN}} = 2.76$ TeV is used for this analysis. General information on the ALICE detector and its performance can be found in [37,38]. The Time Projection Chamber (TPC) [37,39]

and Inner Tracking System (ITS) [37,40] are used to reconstruct charged-particle tracks and measure their momenta with a track-momentum resolution better than 2% for the transverse momentum interval $0.2 < p_T < 5.0$ GeV/c [38]. The two innermost layers of the ITS, the Silicon Pixel Detector (SPD), are employed for triggering and event selection. Two scintillator arrays (V0) [37,41], which cover the pseudorapidity ranges $-3.7 < \eta < -1.7$ (VOC) and $2.8 < \eta < 5.1$ (VOA), are used for triggering, event selection, and the determination of centrality [42] and Ψ_2 . The trigger conditions and the event selection criteria are described in [38]. An offline event selection is applied to remove beam induced background and pileup events. Approximately $9.8 \cdot 10^6$ minimum-bias Pb–Pb events with a reconstructed primary vertex within ± 10 cm from the nominal interaction point in the beam direction belonging to the 0–60% centrality interval are used for this analysis.

Charged particles reconstructed using the combined information from the ITS and TPC in $|\eta| < 0.8$ and $0.2 < p_T < 5.0$ GeV/c are selected with full azimuthal coverage. Additional quality cuts are applied to reduce the contamination from secondary charged particles (i.e. particles originating from weak decays, conversions and secondary hadronic interactions in the detector material) and fake tracks (with random associations of space points). Only tracks with at least 70 space points in the TPC (out of a maximum of 159) with an average χ^2 per degree-of-freedom for the track fit lower than 2, a distance of closest approach (DCA) to the reconstructed event vertex smaller than 2.4 cm in the transverse plane (xy) and 3.2 cm in the longitudinal direction (z) are accepted. The charged particle track reconstruction efficiency was estimated from HIJING simulations [43,44] combined with a GEANT3 [45] detector model, and found to be independent of the collision centrality. The reconstruction efficiency of primary particles defined in [46], which may bias the determination of the p_T averaged charge-dependent correlations and flow, increases from 70% at $p_T = 0.2$ GeV/c to 85% at $p_T \sim 1.5$ GeV/c where it has a maximum. It then gradually decreases and is flat at 80% for $p_T > 3.0$ GeV/c. The systematic uncertainty of the efficiency is about 5%.

The event shape selection is performed as in [30] based on the magnitude of the second-order reduced flow vector, q_2 [47], defined as

$$q_2 = \frac{|\mathbf{Q}_2|}{\sqrt{M}}, \quad (4)$$

where $|\mathbf{Q}_2| = \sqrt{Q_{2,x}^2 + Q_{2,y}^2}$ is the magnitude of the second order harmonic flow vector and M is the multiplicity. The vector \mathbf{Q}_2 is calculated from the azimuthal distribution of the energy deposition measured in the VOC. Its x and y components and the multiplicity are given by

$$Q_{2,x} = \sum_i w_i \cos(2\varphi_i), \quad Q_{2,y} = \sum_i w_i \sin(2\varphi_i), \quad M = \sum_i w_i, \quad (5)$$

where the sum runs over all channels i of the VOC detector ($i = 1 - 32$), φ_i is the azimuthal angle of channel i and w_i is the amplitude measured in channel i . The large gap in pseudorapidity ($|\Delta\eta| > 0.9$) between the charged particles in the TPC used to determine v_2 , $\delta_{\alpha\beta}$ and $\gamma_{\alpha\beta}$ and those in the VOC suppresses non-flow effects. Ten event-shape classes with the lowest (highest) q_2 value corresponding to the 0–10% (90–100%) range are investigated for each centrality interval.

The flow coefficient v_2 is measured using the event plane method [16]. The orientation of the event plane Ψ_2 is estimated from the azimuthal distribution of the energy deposition measured by the VOA detector. The event plane resolution is calculated from correlations between the event planes determined in the TPC and

Table 1

Summary of absolute systematic uncertainties. The uncertainties depend on centrality and shape selection, whose minimum and maximum values are listed here.

	Opposite charge	Same charge
$\delta_{\alpha\beta}$	$(3.4 - 25) \times 10^{-5}$	$(3.1 - 10) \times 10^{-5}$
$\gamma_{\alpha\beta}$	$(2.6 - 34) \times 10^{-6}$	$(4.1 - 74) \times 10^{-6}$
v_2	$(1.2 - 4.7) \times 10^{-3}$	

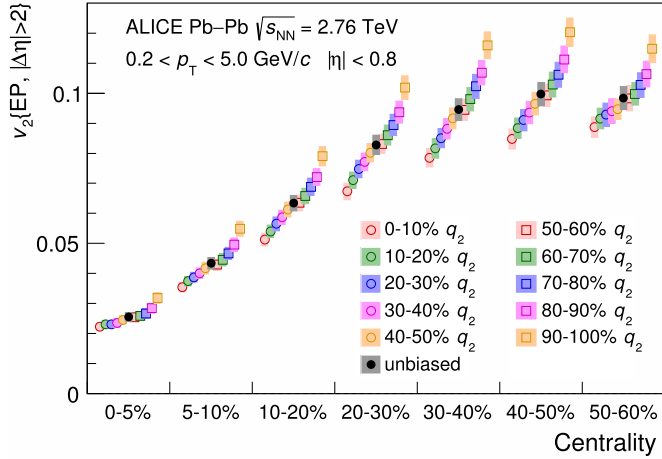


Fig. 1. (Colour online.) Unidentified charged particle v_2 for shape selected and unbiased events as a function of collision centrality. The event selection is based on q_2 determined in the V0C with the lowest (highest) value corresponding to 0–10% (90–100%) q_2 . Points are slightly shifted along the horizontal axis for better visibility. Error bars (shaded boxes) represent the statistical (systematic) uncertainties.

the two V0 detectors separately [16]. The non-flow contributions to the v_2 coefficient and charge-dependent azimuthal correlations are greatly suppressed by the large rapidity separation between the TPC and the VOA ($|\Delta\eta| > 2.0$).

The absolute systematic uncertainties are evaluated from the variation of the results with different selection criteria on the reconstructed collision vertex, different magnetic field polarities, as well as by estimating the centrality from multiplicities measured by the TPC or the SPD rather than the V0 detector. Changes of the results due to variations of the track-selection criteria (e.g. changing the DCA xy and z ranges, number of the TPC space points, using tracks reconstructed by the TPC only) are considered as part of the systematic uncertainties. The effect of reconstruction efficiency on the measurements is checked by randomly rejecting tracks to ensure a flat acceptance in p_T . The detector response is studied using HIJING and AMPT [48] simulations, where the v_2 coefficients and the charge-dependent azimuthal correlations obtained directly from the models are compared with those from reconstructed tracks. The largest contribution to the systematic uncertainties is given by the detector response. The checks related to the reconstruction efficiency, magnetic field polarity and track-selection criteria also yield significant deviations from the nominal values for v_2 , $\gamma_{\alpha\beta}$ and $\delta_{\alpha\beta}$, respectively. The contributions from all sources are added in quadrature as an estimate of the total systematic uncertainty. The resulting systematic uncertainties are summarized in Table 1.

Fig. 1 presents the unidentified charged particle v_2 averaged over $0.2 < p_T < 5.0$ GeV/c for shape selected and unbiased samples as a function of collision centrality. The measured v_2 for the shape selected events differs from the average by up to 25%, which demonstrates that events with the desired initial spatial anisotropy can be experimentally selected. Sensitivity of the event shape selection deteriorates for peripheral collisions (already visible for the

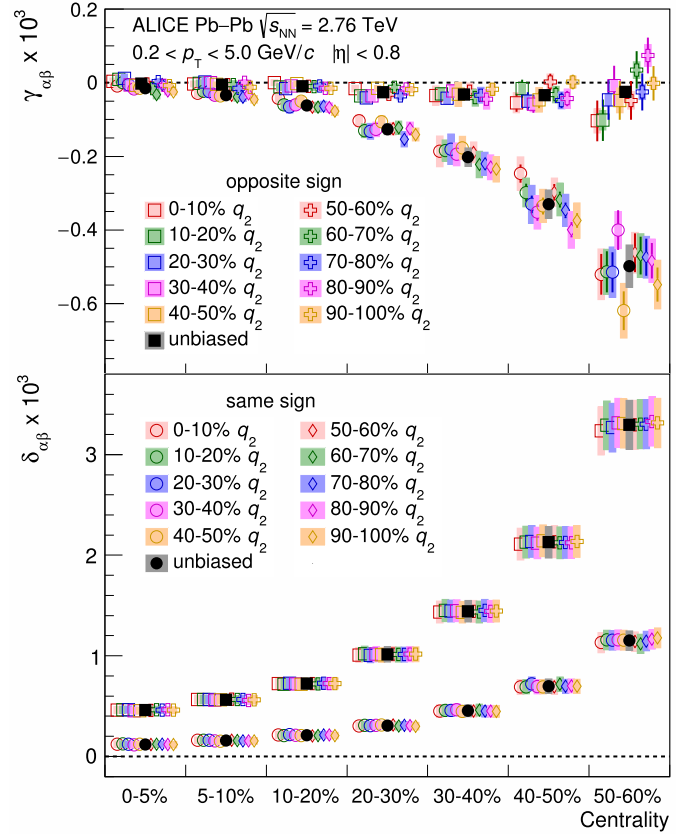


Fig. 2. (Colour online.) Top: Centrality dependence of $\gamma_{\alpha\beta}$ for pairs of particles with same and opposite charge for shape selected and unbiased events. Bottom: Centrality dependence of $\delta_{\alpha\beta}$ for pairs of particles with same and opposite charge for shape selected and unbiased events. The event selection is based on q_2 determined in the V0C with the lowest (highest) value corresponding to 0–10% (90–100%) q_2 . Points are slightly shifted along the horizontal axis for better visibility in both panels. Error bars (shaded boxes) represent the statistical (systematic) uncertainties.

50–60% centrality class) due to the low multiplicity and for central collisions due to the reduced magnitude of flow [30].

The centrality dependence of $\gamma_{\alpha\beta}$ for pairs of particles with same and opposite charge for shape selected and unbiased events is shown in the top panel of Fig. 2. The same charge results denote the average between pairs of particles with only positive and only negative charges since the two combinations are found to be consistent within statistical uncertainties. The correlation of pairs with the same charge is stronger than the correlation for pairs of opposite charge for both shape selected and unbiased events. The ordering of the correlations of pairs with same and opposite charge indicates a charge separation with respect to the reaction plane. The magnitude of the same and opposite charge pair correlations depends weakly on the event-shape selection (q_2 , i.e. v_2) in a given centrality bin.

The bottom panel of Fig. 2 shows the centrality dependence of $\delta_{\alpha\beta}$ for pairs of particles with same and opposite charge for shape selected and unbiased samples. As reported in [27], the magnitude of the correlation for the same charge pairs is smaller than for the opposite charge combinations. This is in contrast to the CME expectation, indicating that background dominates the correlations. The same and opposite charge pair correlations are insensitive to the event-shape selection in a given centrality bin.

The difference between opposite and same charge pair correlations for $\gamma_{\alpha\beta}$ can be used to study the charge separation effect. This difference is presented as a function of v_2 for various centrality classes in the top panel of Fig. 3. The difference is positive

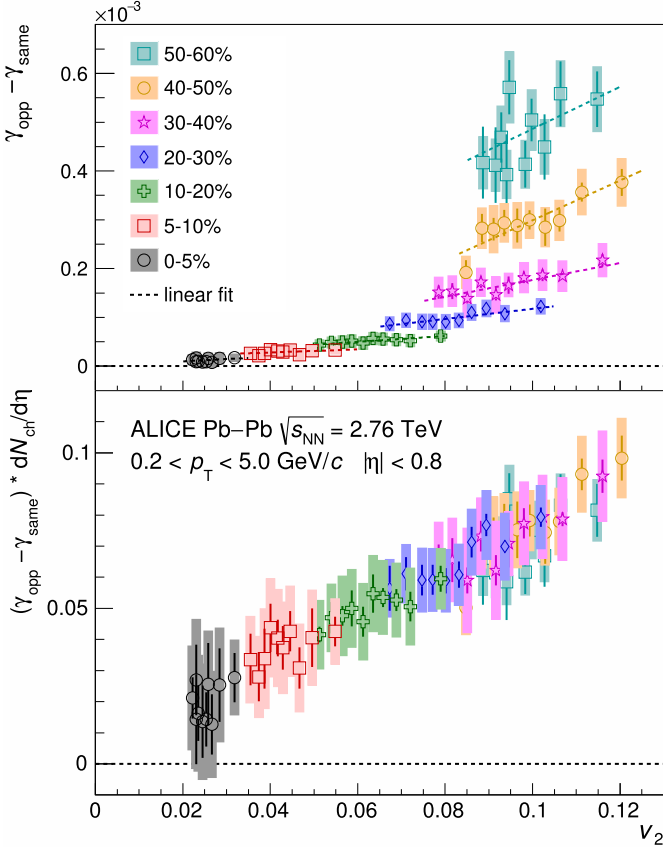


Fig. 3. (Colour online.) Top: Difference between opposite and same charge pair correlations for $\gamma_{\alpha\beta}$ as a function of v_2 for shape selected events together with a linear fit (dashed lines) for various centrality classes. Bottom: Difference between opposite and same charge pair correlations for $\gamma_{\alpha\beta}$ multiplied by the charged-particle density [49] as a function of v_2 for shape selected events for various centrality classes. The event selection is based on q_2 determined in the VOC with the lowest (highest) value corresponding to 0–10% (90–100%) q_2 . Error bars (shaded boxes) represent the statistical (systematic) uncertainties.

for all centralities and its magnitude decreases for more central collisions and with decreasing v_2 (in a given centrality bin). At least two effects could be responsible for the centrality dependence: the reduction of the magnetic field with decreasing centrality and the dilution of the correlation due to the increase in the number of particles [24] in more central collisions. The difference between opposite and same charge pair correlations multiplied by the charged-particle density in a given centrality bin, $dN_{\text{ch}}/d\eta$ (taken from [49]), to compensate for the dilution effect, is presented as a function of v_2 in the bottom panel of Fig. 3. All the data points fall approximately onto the same line. This is qualitatively consistent with expectations from LCC where an increase in v_2 , which modulates the correlation between balancing charges with respect to the reaction plane [50], results in a strong effect. Therefore, the observed dependence on v_2 points to a large background contribution to $\gamma_{\alpha\beta}$.

The expected dependence of the CME signal on v_2 was evaluated with the help of a Monte Carlo Glauber [51] calculation including a magnetic field. In this simulation, the centrality classes are determined from the multiplicity of charged particles in the acceptance of the V0 detector following the method presented in [42]. The multiplicity is generated according to a negative binomial distribution with parameters taken from [42] based on the number of participant nucleons and binary collisions. The elliptic flow is assumed to be proportional to the eccentricity of the participant nucleons and approximately reproduces the measured

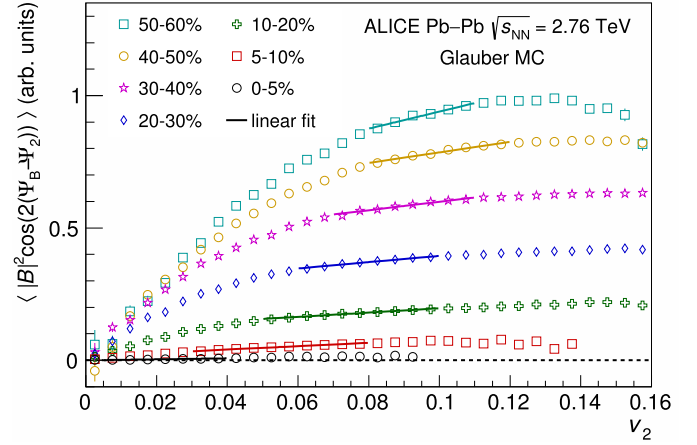


Fig. 4. (Colour online.) The expected dependence of the CME signal on v_2 for various centrality classes from a MC-Glauber simulation [51] (see text for details). No event shape selection is performed in the model, and therefore a large range in v_2 is covered. The solid lines depict linear fits based on the v_2 variation observed within each centrality interval.

p_T -integrated v_2 values [52]. The magnetic field is evaluated at the geometrical centre of the overlap region from the number of spectator nucleons following Eq. (A.6) from [11] with the proper time $\tau = 0.1$ fm/c. The magnetic field is calculated in 1% centrality classes and averaged into the centrality intervals used for data analysis. It is assumed that the CME signal is proportional to $\langle |B|^2 \cos(2(\Psi_B - \Psi_2)) \rangle$, where $|B|$ and Ψ_B are the magnitude and direction of the magnetic field, respectively. Fig. 4 presents the expected dependence of the CME signal on v_2 for various centrality classes. Similar results are found using MC-KLN CGC [53,54] and EKRT [55] initial conditions. The MC-KLN CGC simulation was performed using version 32 of the Monte Carlo k_T -factorization code (*mkt*) available at [56], while the TRENTO model [57] was employed for EKRT initial conditions.

To disentangle the potential CME signal from background, the dependence on v_2 of the difference between opposite and same charge pair correlations for $\gamma_{\alpha\beta}$ and the CME signal expectations are fitted with a linear function (see lines in Figs. 3 (top panel) and 4, respectively):

$$F_1(v_2) = p_0(1 + p_1(v_2 - \langle v_2 \rangle) / \langle v_2 \rangle), \quad (6)$$

where p_0 accounts for the overall scale, which cannot be fixed in the MC calculations, and p_1 reflects the slope normalised such that in a pure background scenario, where the correlator is directly proportional to v_2 , it is equal to unity. The presence of a significant CME contribution, on the other hand, would result in non-zero intercepts at $v_2 = 0$ of the linear functions shown in Fig. 3. The ranges used in these fits are based on the v_2 variation observed in data and the corresponding MC interval within each centrality range. The centrality dependence of p_1 from fits to data and to the signal expectations based on MC-Glauber, MC-KLN CGC and EKRT models is reported in Fig. 5. The observed p_1 from data is a superposition of a possible CME signal and background. Assuming a pure background case, p_1 from data and MC models can be related according to

$$f_{\text{CME}} \times p_{1,\text{MC}} + (1 - f_{\text{CME}}) \times 1 = p_{1,\text{data}}, \quad (7)$$

where f_{CME} denotes the CME fraction to the charge dependence of $\gamma_{\alpha\beta}$ and is given by

$$f_{\text{CME}} = \frac{(\gamma_{\text{opp}} - \gamma_{\text{same}})^{\text{CME}}}{(\gamma_{\text{opp}} - \gamma_{\text{same}})^{\text{CME}} + (\gamma_{\text{opp}} - \gamma_{\text{same}})^{\text{Bkg}}}. \quad (8)$$

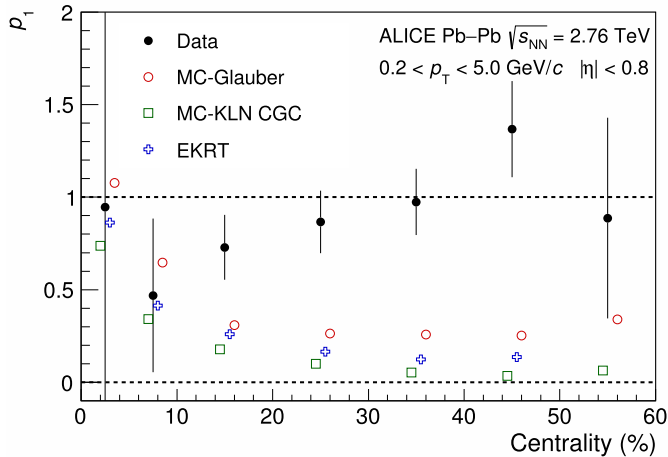


Fig. 5. (Colour online.) Centrality dependence of the p_1 parameter from a linear fit to the difference between opposite and same charge pair correlations for $\gamma_{\alpha\beta}$ and from linear fits to the CME signal expectations from MC-Glauber [51], MC-KLN CGC [53,54] and EKRT [55] models (see text for details). Points from MC simulations are slightly shifted along the horizontal axis for better visibility. Only statistical uncertainties are shown.

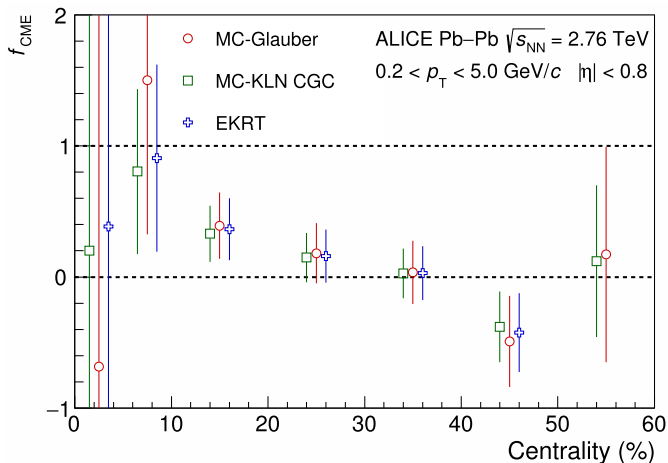


Fig. 6. (Colour online.) Centrality dependence of the CME fraction extracted from the slope parameter of fits to data and MC-Glauber [51], MC-KLN CGC [53,54] and EKRT [55] models, respectively (see text for details). The dashed lines indicate the physical parameter space of the CME fraction. Points are slightly shifted along the horizontal axis for better visibility. Only statistical uncertainties are shown.

Fig. 6 presents f_{CME} for the three models used in this study. The CME fraction cannot be precisely extracted for central (0–10%) and peripheral (50–60%) collisions due to the large statistical uncertainties on p_1 extracted from data. The negative values for the CME fraction obtained for the 40–50% centrality range (deviating from zero by one σ), if confirmed, would indicate that our expectations for the background contribution to be linearly proportional to v_2 are not accurate. Combining the points from 10–50% neglecting a possible centrality dependence gives $f_{\text{CME}} = 0.10 \pm 0.13$, $f_{\text{CME}} = 0.08 \pm 0.10$ and $f_{\text{CME}} = 0.08 \pm 0.11$ for the MC-Glauber, MC-KLN CGC and EKRT models, respectively. These results are consistent with zero CME fraction and correspond to upper limits on f_{CME} of 33%, 26% and 29%, respectively, at 95% confidence level for the 10–50% centrality interval. The CME fraction agrees with the observations in [36] where the centrality intervals overlap.

In summary, the Event Shape Engineering technique has been applied to measure the dependence on v_2 of the charge-dependent two- and three-particle correlators $\delta_{\alpha\beta}$ and $\gamma_{\alpha\beta}$ in Pb–Pb collisions at $\sqrt{s_{\text{NN}}} = 2.76$ TeV. While for $\delta_{\alpha\beta}$ we observe no significant

v_2 dependence in a given centrality bin, $\gamma_{\alpha\beta}$ is found to be almost linearly dependent on v_2 . When the charge dependence of $\gamma_{\alpha\beta}$ is multiplied by the corresponding charged-particle density, to compensate for the dilution effect, a linear dependence on v_2 is observed consistently across all centrality classes. Using a Monte Carlo simulation with different initial-state models, we have found that the CME signal is expected to exhibit a weak dependence on v_2 in the measured range. The observations imply that the dominant contribution to $\gamma_{\alpha\beta}$ is due to non-CME effects. In order to get a quantitative estimate of the signal and background contributions to the measurements, we fit both $\gamma_{\alpha\beta}$ and the expected signal dependence on v_2 with a first order polynomial. This procedure allows to estimate the fraction of the CME signal in the centrality range 10–50%, but not for the most central (0–10%) and peripheral (50–60%) collisions due to large statistical uncertainties. Averaging over the centrality range 10–50% gives an upper limit of 26% to 33% (depending on the initial-state model) at 95% confidence level for the CME contribution to the difference between opposite and same charge pair correlations for $\gamma_{\alpha\beta}$.

Acknowledgements

The ALICE Collaboration would like to thank all its engineers and technicians for their invaluable contributions to the construction of the experiment and the CERN accelerator teams for the outstanding performance of the LHC complex. The ALICE Collaboration gratefully acknowledges the resources and support provided by all Grid centres and the Worldwide LHC Computing Grid (WLCG) collaboration. The ALICE Collaboration acknowledges the following funding agencies for their support in building and running the ALICE detector: A.I. Alikhanyan National Science Laboratory (Yerevan Physics Institute) Foundation (ANSL), State Committee of Science and World Federation of Scientists (WFS), Armenia; Austrian Academy of Sciences and Nationalstiftung für Forschung, Technologie und Entwicklung, Austria; Ministry of Communications and High Technologies, National Nuclear Research Center, Azerbaijan; Conselho Nacional de Desenvolvimento Científico e Tecnológico (CNPq), Universidade Federal do Rio Grande do Sul (UFRGS), Financiadora de Estudos e Projetos (Finep) and Fundação de Amparo à Pesquisa do Estado de São Paulo (FAPESP), Brazil; Ministry of Science & Technology of China (MSTC), National Natural Science Foundation of China (NSFC) and Ministry of Education of China (MOEC), China; Ministry of Science, Education and Sport and Croatian Science Foundation, Croatia; Ministry of Education, Youth and Sports of the Czech Republic, Czech Republic; The Danish Council for Independent Research – Natural Sciences, the Carlsberg Foundation and Danish National Research Foundation (DNRF), Denmark; Helsinki Institute of Physics (HIP), Finland; Commissariat à l’Energie Atomique (CEA) and Institut National de Physique Nucléaire et de Physique des Particules (IN2P3) and Centre National de la Recherche Scientifique (CNRS), France; Bundesministerium für Bildung, Wissenschaft, Forschung und Technologie (BMBF) and GSI Helmholtzzentrum für Schwerionenforschung GmbH, Germany; General Secretariat for Research and Technology, Ministry of Education, Research and Religions, Greece; National Research, Development and Innovation Office, Hungary; Department of Atomic Energy, Government of India (DAE) and Council of Scientific and Industrial Research (CSIR), New Delhi, India; Indonesian Institute of Science, Indonesia; Centro Fermi – Museo Storico della Fisica e Centro Studi e Ricerche Enrico Fermi and Istituto Nazionale di Fisica Nucleare (INFN), Italy; Institute for Innovative Science and Technology, Nagasaki Institute of Applied Science (IIST), Japan Society for the Promotion of Science (JSPS) KAKENHI and Japanese Ministry of Education, Culture, Sports, Science and Technology (MEXT), Japan; Consejo Nacional

de Ciencia (CONACYT) y Tecnología, through Fondo de Cooperación Internacional en Ciencia y Tecnología (FONCICYT) and Dirección General de Asuntos del Personal Académico (DGAPA), Mexico; Nederlandse Organisatie voor Wetenschappelijk Onderzoek (NWO), Netherlands; The Research Council of Norway, Norway; Commission on Science and Technology for Sustainable Development in the South (COMSATS), Pakistan; Pontificia Universidad Católica del Perú, Peru; Ministry of Science and Higher Education and National Science Centre, Poland; Korea Institute of Science and Technology Information and National Research Foundation of Korea (NRF), Republic of Korea; Ministry of Education and Scientific Research, Institute of Atomic Physics and Romanian National Agency for Science, Technology and Innovation, Romania; Joint Institute for Nuclear Research (JINR), Ministry of Education and Science of the Russian Federation and National Research Centre Kurchatov Institute, Russia; Ministry of Education, Science, Research and Sport of the Slovak Republic, Slovakia; National Research Foundation of South Africa, South Africa; Centro de Aplicaciones Tecnológicas y Desarrollo Nuclear (CEADEN), Cubaenergía, Cuba, Ministerio de Ciencia e Innovación and Centro de Investigaciones Energéticas, Medioambientales y Tecnológicas (CIEMAT), Spain; Swedish Research Council (VR) and Knut & Alice Wallenberg Foundation (KAW), Sweden; European Organization for Nuclear Research, Switzerland; National Science and Technology Development Agency (NSDTA), Suranaree University of Technology (SUT) and Office of the Higher Education Commission under NRU project of Thailand, Thailand; Turkish Atomic Energy Agency (TAEK), Turkey; National Academy of Sciences of Ukraine, Ukraine; Science and Technology Facilities Council (STFC), United Kingdom; National Science Foundation of the United States of America (NSF) and U.S. Department of Energy, Office of Nuclear Physics (DOE NP), United States of America.

References

- [1] T.D. Lee, A theory of spontaneous T violation, *Phys. Rev. D* 8 (1973) 1226–1239.
- [2] T.D. Lee, G.C. Wick, Vacuum stability and vacuum excitation in a spin 0 field theory, *Phys. Rev. D* 9 (1974) 2291–2316.
- [3] P.D. Morley, I.A. Schmidt, Strong P, CP, T violations in heavy ion collisions, *Z. Phys. C* 26 (1985) 627.
- [4] D. Kharzeev, R.D. Pisarski, M.H.G. Tytgat, Possibility of spontaneous parity violation in hot QCD, *Phys. Rev. Lett.* 81 (1998) 512–515, arXiv:hep-ph/9804221.
- [5] S.-S. Chern, J. Simons, Characteristic forms and geometric invariants, *Ann. Math.* 99 (1974) 48–69.
- [6] A. Bzdak, V. Skokov, Event-by-event fluctuations of magnetic and electric fields in heavy ion collisions, *Phys. Lett. B* 710 (2012) 171–174, arXiv:1111.1949 [hep-ph].
- [7] W.-T. Deng, X.-G. Huang, Event-by-event generation of electromagnetic fields in heavy-ion collisions, *Phys. Rev. C* 85 (2012) 044907, arXiv:1201.5108 [nucl-th].
- [8] U. Gursoy, D. Kharzeev, K. Rajagopal, Magnetohydrodynamics, charged currents and directed flow in heavy ion collisions, *Phys. Rev. C* 89 (5) (2014) 054905, arXiv:1401.3805 [hep-ph].
- [9] D. Kharzeev, Parity violation in hot QCD: why it can happen, and how to look for it, *Phys. Lett. B* 633 (2006) 260–264, arXiv:hep-ph/0406125.
- [10] D. Kharzeev, A. Zhitnitsky, Charge separation induced by P-odd bubbles in QCD matter, *Nucl. Phys. A* 797 (2007) 67–79, arXiv:0706.1026 [hep-ph].
- [11] D.E. Kharzeev, L.D. McLerran, H.J. Warringa, The effects of topological charge change in heavy ion collisions: 'event by event P and CP violation', *Nucl. Phys. A* 803 (2008) 227–253, arXiv:0711.0950 [hep-ph].
- [12] K. Fukushima, D.E. Kharzeev, H.J. Warringa, The chiral magnetic effect, *Phys. Rev. D* 78 (2008) 074033, arXiv:0808.3382 [hep-ph].
- [13] S.A. Voloshin, A.M. Poskanzer, R. Snellings, Collective phenomena in non-central nuclear collisions, arXiv:0809.2949 [nucl-ex].
- [14] U. Heinz, R. Snellings, Collective flow and viscosity in relativistic heavy-ion collisions, *Annu. Rev. Nucl. Part. Sci.* 63 (2013) 123–151, arXiv:1301.2826 [nucl-th].
- [15] S. Voloshin, Y. Zhang, Flow study in relativistic nuclear collisions by Fourier expansion of Azimuthal particle distributions, *Z. Phys. C* 70 (1996) 665–672, arXiv:hep-ph/9407282.
- [16] A.M. Poskanzer, S.A. Voloshin, Methods for analyzing anisotropic flow in relativistic nuclear collisions, *Phys. Rev. C* 58 (1998) 1671–1678, arXiv:nucl-ex/9805001.
- [17] S.A. Voloshin, Parity violation in hot QCD: how to detect it, *Phys. Rev. C* 70 (2004) 057901, arXiv:hep-ph/0406311.
- [18] S. Schlichting, S. Pratt, Charge conservation at energies available at the BNL Relativistic Heavy Ion Collider and contributions to local parity violation observables, *Phys. Rev. C* 83 (2011) 014913, arXiv:1009.4283 [nucl-th].
- [19] S. Pratt, S. Schlichting, S. Gavin, Effects of momentum conservation and flow on angular correlations at RHIC, *Phys. Rev. C* 84 (2011) 024909, arXiv:1011.6053 [nucl-th].
- [20] J. Liao, V. Koch, A. Bzdak, On the charge separation effect in relativistic heavy ion collisions, *Phys. Rev. C* 82 (2010) 054902, arXiv:1005.5380 [nucl-th].
- [21] A. Bzdak, V. Koch, J. Liao, Azimuthal correlations from transverse momentum conservation and possible local parity violation, *Phys. Rev. C* 83 (2011) 014905, arXiv:1008.4919 [nucl-th].
- [22] D. Teaney, L. Yan, Triangularity and dipole asymmetry in heavy ion collisions, *Phys. Rev. C* 83 (2011) 064904, arXiv:1010.1876 [nucl-th].
- [23] STAR Collaboration, B.I. Abelev, et al., Azimuthal charged-particle correlations and possible local strong parity violation, *Phys. Rev. Lett.* 103 (2009) 251601, arXiv:0909.1739 [nucl-ex].
- [24] STAR Collaboration, B.I. Abelev, et al., Observation of charge-dependent azimuthal correlations and possible local strong parity violation in heavy ion collisions, *Phys. Rev. C* 81 (2010) 054908, arXiv:0909.1717 [nucl-ex].
- [25] STAR Collaboration, L. Adamczyk, et al., Fluctuations of charge separation perpendicular to the event plane and local parity violation in $\sqrt{s_{NN}} = 200$ GeV Au+Au collisions at the BNL Relativistic Heavy Ion Collider, *Phys. Rev. C* 88 (6) (2013) 064911, arXiv:1302.3802 [nucl-ex].
- [26] STAR Collaboration, L. Adamczyk, et al., Beam-energy dependence of charge separation along the magnetic field in Au+Au collisions at RHIC, *Phys. Rev. Lett.* 113 (2014) 052302, arXiv:1404.1433 [nucl-ex].
- [27] ALICE Collaboration, B. Abelev, et al., Charge separation relative to the reaction plane in Pb–Pb collisions at $\sqrt{s_{NN}} = 2.76$ TeV, *Phys. Rev. Lett.* 110 (1) (2013) 012301, arXiv:1207.0900 [nucl-ex].
- [28] ALICE Collaboration, J. Adam, et al., Charge-dependent flow and the search for the chiral magnetic wave in Pb–Pb collisions at $\sqrt{s_{NN}} = 2.76$ TeV, *Phys. Rev. C* 93 (4) (2016) 044903, arXiv:1512.05739 [nucl-ex].
- [29] J. Schukraft, A. Timmins, S.A. Voloshin, Ultra-relativistic nuclear collisions: event shape engineering, *Phys. Lett. B* 719 (2013) 394–398, arXiv:1208.4563 [nucl-ex].
- [30] ALICE Collaboration, J. Adam, et al., Event shape engineering for inclusive spectra and elliptic flow in Pb–Pb collisions at $\sqrt{s_{NN}} = 2.76$ TeV, *Phys. Rev. C* 93 (3) (2016) 034916, arXiv:1507.06194 [nucl-ex].
- [31] ATLAS Collaboration, G. Aad, et al., Measurement of the correlation between flow harmonics of different order in lead-lead collisions at $\sqrt{s_{NN}} = 2.76$ TeV with the ATLAS detector, *Phys. Rev. C* 92 (3) (2015) 034903, arXiv:1504.01289 [hep-ex].
- [32] F.G. Gardim, F. Grassi, M. Luzum, J.-Y. Ollitrault, Mapping the hydrodynamic response to the initial geometry in heavy-ion collisions, *Phys. Rev. C* 85 (2012) 024908, arXiv:1111.6538 [nucl-th].
- [33] A. Bzdak, Suppression of elliptic flow induced correlations in an observable of possible local parity violation, *Phys. Rev. C* 85 (2012) 044919, arXiv:1112.4066 [nucl-th].
- [34] CMS Collaboration, V. Khachatryan, et al., Observation of charge-dependent azimuthal correlations in p–Pb collisions and its implication for the search for the chiral magnetic effect, *Phys. Rev. Lett.* 118 (12) (2017) 122301, arXiv:1610.00263 [nucl-ex].
- [35] R. Belmont, J.L. Nagle, To CME or not to CME? Implications of p+Pb measurements of the chiral magnetic effect in heavy ion collisions, *Phys. Rev. C* 96 (2) (2017) 024901, arXiv:1610.07964 [nucl-th].
- [36] CMS Collaboration, A.M. Sirunyan, et al., Constraints on the chiral magnetic effect using charge-dependent azimuthal correlations in pPb and PbPb collisions at the LHC, arXiv:1708.01602 [nucl-ex].
- [37] ALICE Collaboration, K. Aamodt, et al., The ALICE experiment at the CERN LHC, *J. Instrum.* 3 (2008) S08002.
- [38] ALICE Collaboration, B.B. Abelev, et al., Performance of the ALICE experiment at the CERN LHC, *Int. J. Mod. Phys. A* 29 (2014) 1430044, arXiv:1402.4476 [nucl-ex].
- [39] J. Alme, et al., The ALICE TPC, a large 3-dimensional tracking device with fast readout for ultra-high multiplicity events, *Nucl. Instrum. Methods Phys. Res., Sect. A, Accel. Spectrom. Detect. Assoc. Equip.* 622 (2010) 316–367, arXiv:1001.1950 [physics.ins-det].
- [40] ALICE Collaboration, K. Aamodt, et al., Alignment of the ALICE Inner Tracking System with cosmic-ray tracks, *J. Instrum.* 5 (2010) P03003, arXiv:1001.0502 [physics.ins-det].
- [41] ALICE Collaboration, E. Abbas, et al., Performance of the ALICE VZERO system, *J. Instrum.* 8 (2013) P10016, arXiv:1306.3130 [nucl-ex].
- [42] ALICE Collaboration, B. Abelev, et al., Centrality determination of Pb–Pb collisions at $\sqrt{s_{NN}} = 2.76$ TeV with ALICE, *Phys. Rev. C* 88 (4) (2013) 044909, arXiv:1301.4361 [nucl-ex].
- [43] X.-N. Wang, M. Gyulassy, HIJING: a Monte Carlo model for multiple jet production in p, p, p A and A A collisions, *Phys. Rev. D* 44 (1991) 3501–3516.
- [44] M. Gyulassy, X.-N. Wang, HIJING 1.0: a Monte Carlo program for parton and particle production in high-energy hadronic and nuclear collisions, *Comput. Phys. Commun.* 83 (1994) 307, arXiv:nucl-th/9502021.

- [45] R. Brun, F. Bruyant, F. Carminati, S. Giani, M. Maire, A. McPherson, G. Patrick, L. Urban, GEANT detector description and simulation tool, CERN-W5013 1 (1994) 1.
- [46] ALICE Collaboration, S. Acharya, et al., The ALICE definition of primary particles, ALICE-PUBLIC-2017-005, <https://cds.cern.ch/record/2270008>.
- [47] STAR Collaboration, C. Adler, et al., Elliptic flow from two and four particle correlations in Au+Au collisions at $\sqrt{s_{NN}} = 130$ GeV, Phys. Rev. C 66 (2002) 034904, arXiv:nucl-ex/0206001.
- [48] Z.-W. Lin, C.M. Ko, B.-A. Li, B. Zhang, S. Pal, A multi-phase transport model for relativistic heavy ion collisions, Phys. Rev. C 72 (2005) 064901, arXiv:nucl-th/0411110.
- [49] ALICE Collaboration, K. Aamodt, et al., Centrality dependence of the charged-particle multiplicity density at mid-rapidity in Pb–Pb collisions at $\sqrt{s_{NN}} = 2.76$ TeV, Phys. Rev. Lett. 106 (2011) 032301, arXiv:1012.1657 [nucl-ex].
- [50] Y. Hori, T. Gunji, H. Hamagaki, S. Schlichting, Collective flow effects on charge balance correlations and local parity-violation observables in $\sqrt{s_{NN}} = 2.76$ TeV Pb+Pb collisions at the LHC, arXiv:1208.0603 [nucl-th].
- [51] M.L. Miller, K. Reygers, S.J. Sanders, P. Steinberg, Glauber modeling in high energy nuclear collisions, Annu. Rev. Nucl. Part. Sci. 57 (2007) 205–243, arXiv:nucl-ex/0701025.
- [52] ALICE Collaboration, K. Aamodt, et al., Elliptic flow of charged particles in Pb–Pb collisions at 2.76 TeV, Phys. Rev. Lett. 105 (2010) 252302, arXiv:1011.3914 [nucl-ex].
- [53] H.-J. Drescher, Y. Nara, Eccentricity fluctuations from the color glass condensate at RHIC and LHC, Phys. Rev. C 76 (2007) 041903, arXiv:0707.0249 [nucl-th].
- [54] J.L. Albacete, A. Dumitru, A model for gluon production in heavy-ion collisions at the LHC with rcBK unintegrated gluon densities, arXiv:1011.5161 [hep-ph].
- [55] H. Niemi, K.J. Eskola, R. Paatelainen, Event-by-event fluctuations in a perturbative QCD + saturation + hydrodynamics model: determining QCD matter shear viscosity in ultrarelativistic heavy-ion collisions, Phys. Rev. C 93 (2) (2016) 024907, arXiv:1505.02677 [hep-ph].
- [56] http://faculty.baruch.cuny.edu/naturalscience/physics/dumitru/CGC_IC.html.
- [57] J.S. Moreland, J.E. Bernhard, S.A. Bass, Alternative ansatz to wounded nucleon and binary collision scaling in high-energy nuclear collisions, Phys. Rev. C 92 (1) (2015) 011901, arXiv:1412.4708 [nucl-th].

ALICE Collaboration

S. Acharya¹³⁹, J. Adam⁹⁸, D. Adamová⁹⁵, J. Adolfsson³⁴, M.M. Aggarwal¹⁰⁰, G. Aglieri Rinella³⁵, M. Agnello³¹, N. Agrawal⁴⁸, Z. Ahammed¹³⁹, N. Ahmad¹⁷, S.U. Ahn⁸⁰, S. Aiola¹⁴³, A. Akindinov⁶⁵, M. Al-Turany¹⁰⁸, S.N. Alam¹³⁹, D.S.D. Albuquerque¹²⁴, D. Aleksandrov⁹¹, B. Alessandro⁵⁹, R. Alfaro Molina⁷⁵, A. Alici^{27,54,12}, A. Alkin³, J. Alme²², T. Alt⁷¹, L. Altenkamper²², I. Altsybeev¹³⁸, C. Alves Garcia Prado¹²³, C. Andrei⁸⁸, D. Andreou³⁵, H.A. Andrews¹¹², A. Andronic¹⁰⁸, V. Anguelov¹⁰⁵, C. Anson⁹⁸, T. Antičić¹⁰⁹, F. Antinori⁵⁷, P. Antonioli⁵⁴, R. Anwar¹²⁶, L. Aphecetche¹¹⁶, H. Appelshäuser⁷¹, S. Arcelli²⁷, R. Arnaldi⁵⁹, O.W. Arnold^{106,36}, I.C. Arsene²¹, M. Arslanodok¹⁰⁵, B. Audurier¹¹⁶, A. Augustinus³⁵, R. Averbeck¹⁰⁸, M.D. Azmi¹⁷, A. Badalà⁵⁶, Y.W. Baek^{61,79}, S. Bagnasco⁵⁹, R. Bailhache⁷¹, R. Bala¹⁰², A. Baldisseri⁷⁶, M. Ball⁴⁵, R.C. Baral^{68,89}, A.M. Barbano²⁶, R. Barbera²⁸, F. Barile^{53,33}, L. Barioglio²⁶, G.G. Barnaföldi¹⁴², L.S. Barnby⁹⁴, V. Barret¹³³, P. Bartalini⁷, K. Barth³⁵, E. Bartsch⁷¹, M. Basile²⁷, N. Bastid¹³³, S. Basu¹⁴¹, G. Batigne¹¹⁶, B. Batyunya⁷⁸, P.C. Batzing²¹, J.L. Bazo Alba¹¹³, I.G. Bearden⁹², H. Beck¹⁰⁵, C. Bedda⁶⁴, N.K. Behera⁶¹, I. Belikov¹³⁵, F. Bellini^{27,35}, H. Bello Martinez², R. Bellwied¹²⁶, L.G.E. Beltran¹²², V. Belyaev⁸⁴, G. Bencedi¹⁴², S. Beole²⁶, A. Bercuci⁸⁸, Y. Berdnikov⁹⁷, D. Berenyi¹⁴², R.A. Bertens¹²⁹, D. Berzano³⁵, L. Betev³⁵, A. Bhasin¹⁰², I.R. Bhat¹⁰², A.K. Bhati¹⁰⁰, B. Bhattacharjee⁴⁴, J. Bhom¹²⁰, A. Bianchi²⁶, L. Bianchi¹²⁶, N. Bianchi⁵¹, C. Bianchin¹⁴¹, J. Bielčík³⁹, J. Bielčíková⁹⁵, A. Bilandzic^{36,106}, G. Biro¹⁴², R. Biswas⁴, S. Biswas⁴, J.T. Blair¹²¹, D. Blau⁹¹, C. Blume⁷¹, G. Boca¹³⁶, F. Bock^{83,35,105}, A. Bogdanov⁸⁴, L. Boldizsár¹⁴², M. Bombara⁴⁰, G. Bonomi¹³⁷, M. Bonora³⁵, J. Book⁷¹, H. Borel⁷⁶, A. Borissov^{105,19}, M. Borri¹²⁸, E. Botta²⁶, C. Bourjau⁹², L. Bratrud⁷¹, P. Braun-Munzinger¹⁰⁸, M. Bregant¹²³, T.A. Broker⁷¹, M. Broz³⁹, E.J. Brucken⁴⁶, E. Bruna⁵⁹, G.E. Bruno^{35,33}, D. Budnikov¹¹⁰, H. Buesching⁷¹, S. Bufalino³¹, P. Buhler¹¹⁵, P. Buncic³⁵, O. Busch¹³², Z. Buthelezi⁷⁷, J.B. Butt¹⁵, J.T. Buxton¹⁸, J. Cabala¹¹⁸, D. Caffarri^{35,93}, H. Caines¹⁴³, A. Caliva^{64,108}, E. Calvo Villar¹¹³, P. Camerini²⁵, A.A. Capon¹¹⁵, F. Carena³⁵, W. Carena³⁵, F. Carnesecchi^{27,12}, J. Castillo Castellanos⁷⁶, A.J. Castro¹²⁹, E.A.R. Casula⁵⁵, C. Ceballos Sanchez⁹, P. Cerello⁵⁹, S. Chandra¹³⁹, B. Chang¹²⁷, S. Chapeland³⁵, M. Chartier¹²⁸, S. Chattopadhyay¹³⁹, S. Chattopadhyay¹¹¹, A. Chauvin^{36,106}, C. Cheshkov¹³⁴, B. Cheynis¹³⁴, V. Chibante Barroso³⁵, D.D. Chinellato¹²⁴, S. Cho⁶¹, P. Chochula³⁵, M. Chojnacki⁹², S. Choudhury¹³⁹, T. Chowdhury¹³³, P. Christakoglou⁹³, C.H. Christensen⁹², P. Christiansen³⁴, T. Chujo¹³², S.U. Chung¹⁹, C. Cicalo⁵⁵, L. Cifarelli^{12,27}, F. Cindolo⁵⁴, J. Cleymans¹⁰¹, F. Colamaria³³, D. Colella^{35,66,53}, A. Collu⁸³, M. Colocci²⁷, M. Concas^{59,ii}, G. Conesa Balbastre⁸², Z. Conesa del Valle⁶², M.E. Connors^{143,iii}, J.G. Contreras³⁹, T.M. Cormier⁹⁶, Y. Corrales Morales⁵⁹, I. Cortés Maldonado², P. Cortese³², M.R. Cosentino¹²⁵, F. Costa³⁵, S. Costanza¹³⁶, J. Crkovská⁶², P. Crochet¹³³, E. Cuautle⁷³, L. Cunqueiro⁷², T. Dahms^{36,106}, A. Dainese⁵⁷, M.C. Danisch¹⁰⁵, A. Danu⁶⁹, D. Das¹¹¹, I. Das¹¹¹, S. Das⁴, A. Dash⁸⁹, S. Dash⁴⁸, S. De^{49,123}, A. De Caro³⁰, G. de Cataldo⁵³, C. de Conti¹²³, J. de Cuveland⁴², A. De Falco²⁴, D. De Gruttola^{30,12}, N. De Marco⁵⁹, S. De Pasquale³⁰, R.D. De Souza¹²⁴, H.F. Degenhardt¹²³, A. Deisting^{108,105}, A. Deloff⁸⁷, C. Deplano⁹³, P. Dhankher⁴⁸, D. Di Bari³³, A. Di Mauro³⁵, P. Di Nezza⁵¹, B. Di Ruzza⁵⁷, M.A. Diaz Corchero¹⁰, T. Dietel¹⁰¹, P. Dillenseger⁷¹, R. Divià³⁵, Ø. Djuvsland²², A. Dobrin³⁵, D. Domenicis Gimenez¹²³, B. Dönigus⁷¹, O. Dordic²¹, L.V.R. Doremalen⁶⁴, A.K. Dubey¹³⁹,

A. Dubla¹⁰⁸, L. Ducroux¹³⁴, A.K. Duggal¹⁰⁰, M. Dukhishyam⁸⁹, P. Dupieux¹³³, R.J. Ehlers¹⁴³, D. Elia⁵³,
 E. Endress¹¹³, H. Engel⁷⁰, E. Eppele¹⁴³, B. Erazmus¹¹⁶, F. Erhardt⁹⁹, B. Espagnon⁶², S. Esumi¹³²,
 G. Eulisse³⁵, J. Eum¹⁹, D. Evans¹¹², S. Evdokimov¹¹⁴, L. Fabbietti^{106,36}, J. Faivre⁸², A. Fantoni⁵¹,
 M. Fasel^{96,83}, L. Feldkamp⁷², A. Feliciello⁵⁹, G. Feofilov¹³⁸, A. Fernández Téllez², E.G. Ferreira¹⁶,
 A. Ferretti²⁶, A. Festanti^{29,35}, V.J.G. Feuillard^{76,133}, J. Figiel¹²⁰, M.A.S. Figueredo¹²³, S. Filchagin¹¹⁰,
 D. Finogeev⁶³, F.M. Fionda^{22,24}, M. Floris³⁵, S. Foertsch⁷⁷, P. Foka¹⁰⁸, S. Fokin⁹¹, E. Fragiaco⁶⁰,
 A. Francescon³⁵, A. Francisco¹¹⁶, U. Frankenfeld¹⁰⁸, G.G. Fronze²⁶, U. Fuchs³⁵, C. Furget⁸², A. Furs⁶³,
 M. Fusco Girard³⁰, J.J. Gaardhøje⁹², M. Gagliardi²⁶, A.M. Gago¹¹³, K. Gajdosova⁹², M. Gallio²⁶,
 C.D. Galvan¹²², P. Ganoti⁸⁶, C. Garabatos¹⁰⁸, E. Garcia-Solis¹³, K. Garg²⁸, C. Gargiulo³⁵, P. Gasik^{106,36},
 E.F. Gauger¹²¹, M.B. Gay Ducati⁷⁴, M. Germain¹¹⁶, J. Ghosh¹¹¹, P. Ghosh¹³⁹, S.K. Ghosh⁴, P. Gianotti⁵¹,
 P. Giubellino^{35,108,59}, P. Giubilato²⁹, E. Gladysz-Dziadus¹²⁰, P. Glässel¹⁰⁵, D.M. Gómez Coral⁷⁵,
 A. Gomez Ramirez⁷⁰, A.S. Gonzalez³⁵, V. Gonzalez¹⁰, P. González-Zamora^{10,2}, S. Gorbunov⁴²,
 L. Görlich¹²⁰, S. Gotovac¹¹⁹, V. Grabski⁷⁵, L.K. Graczykowski¹⁴⁰, K.L. Graham¹¹², L. Greiner⁸³,
 A. Grelli⁶⁴, C. Grigoras³⁵, V. Grigoriev⁸⁴, A. Grigoryan¹, S. Grigoryan⁷⁸, J.M. Gronefeld¹⁰⁸, F. Grosa³¹,
 J.F. Grosse-Oetringhaus³⁵, R. Grosso¹⁰⁸, L. Gruber¹¹⁵, F. Guber⁶³, R. Guernane⁸², B. Guerzoni²⁷,
 K. Gulbrandsen⁹², T. Gunji¹³¹, A. Gupta¹⁰², R. Gupta¹⁰², I.B. Guzman², R. Haake³⁵, C. Hadjidakis⁶²,
 H. Hamagaki⁸⁵, G. Hamar¹⁴², J.C. Hamon¹³⁵, M.R. Haque⁶⁴, J.W. Harris¹⁴³, A. Harton¹³, H. Hassan⁸²,
 D. Hatzifotiadou^{12,54}, S. Hayashi¹³¹, S.T. Heckel⁷¹, E. Hellbär⁷¹, H. Helstrup³⁷, A. Herghelegiu⁸⁸,
 E.G. Hernandez², G. Herrera Corral¹¹, F. Herrmann⁷², B.A. Hess¹⁰⁴, K.F. Hetland³⁷, H. Hillemanns³⁵,
 C. Hills¹²⁸, B. Hippolyte¹³⁵, J. Hladky⁶⁷, B. Hohlweger¹⁰⁶, D. Horak³⁹, S. Hornung¹⁰⁸,
 R. Hosokawa^{82,132}, P. Hristov³⁵, C. Hughes¹²⁹, T.J. Humanic¹⁸, N. Hussain⁴⁴, T. Hussain¹⁷, D. Hutter⁴²,
 D.S. Hwang²⁰, S.A. Iga Buitron⁷³, R. Ilkaev¹¹⁰, M. Inaba¹³², M. Ippolitov^{84,91}, M. Irfan¹⁷, M.S. Islam¹¹¹,
 M. Ivanov¹⁰⁸, V. Ivanov⁹⁷, V. Izucheev¹¹⁴, B. Jacak⁸³, N. Jacazio²⁷, P.M. Jacobs⁸³, M.B. Jadhav⁴⁸,
 J. Jadlovsky¹¹⁸, S. Jaelani⁶⁴, C. Jahnke³⁶, M.J. Jakubowska¹⁴⁰, M.A. Janik¹⁴⁰, P.H.S.Y. Jayarathna¹²⁶,
 C. Jena⁸⁹, S. Jena¹²⁶, M. Jercic⁹⁹, R.T. Jimenez Bustamante¹⁰⁸, P.G. Jones¹¹², A. Jusko¹¹², P. Kalinak⁶⁶,
 A. Kalweit³⁵, J.H. Kang¹⁴⁴, V. Kaplin⁸⁴, S. Kar¹³⁹, A. Karasu Uysal⁸¹, O. Karavichev⁶³, T. Karavicheva⁶³,
 L. Karayan^{108,105}, P. Karczmarczyk³⁵, E. Karpechev⁶³, U. Kebschull⁷⁰, R. Keidel¹⁴⁵, D.L.D. Keijdener⁶⁴,
 M. Keil³⁵, B. Ketzer⁴⁵, Z. Khabanova⁹³, P. Khan¹¹¹, S.A. Khan¹³⁹, A. Khanzadeev⁹⁷, Y. Kharlov¹¹⁴,
 A. Khatun¹⁷, A. Khuntia⁴⁹, M.M. Kielbowicz¹²⁰, B. Kileng³⁷, B. Kim¹³², D. Kim¹⁴⁴, D.J. Kim¹²⁷,
 H. Kim¹⁴⁴, J.S. Kim⁴³, J. Kim¹⁰⁵, M. Kim⁶¹, M. Kim¹⁴⁴, S. Kim²⁰, T. Kim¹⁴⁴, S. Kirsch⁴², I. Kisel⁴²,
 S. Kiselev⁶⁵, A. Kisiel¹⁴⁰, G. Kiss¹⁴², J.L. Klay⁶, C. Klein⁷¹, J. Klein³⁵, C. Klein-Bösing⁷², S. Klewin¹⁰⁵,
 A. Kluge³⁵, M.L. Knichel^{35,105}, A.G. Knospe¹²⁶, C. Kobdaj¹¹⁷, M. Kofarago¹⁴², M.K. Köhler¹⁰⁵,
 T. Kollegger¹⁰⁸, V. Kondratiev¹³⁸, N. Kondratyeva⁸⁴, E. Kondratyuk¹¹⁴, A. Konevskikh⁶³,
 M. Konyushikhin¹⁴¹, M. Kopcik¹¹⁸, M. Kour¹⁰², C. Kouzinopoulos³⁵, O. Kovalenko⁸⁷, V. Kovalenko¹³⁸,
 M. Kowalski¹²⁰, G. Koyithatta Meethaleveedu⁴⁸, I. Králik⁶⁶, A. Kravčáková⁴⁰, L. Kreis¹⁰⁸,
 M. Krivda^{66,112}, F. Krizek⁹⁵, E. Kryshen⁹⁷, M. Krzewicki⁴², A.M. Kubera¹⁸, V. Kučera⁹⁵, C. Kuhn¹³⁵,
 P.G. Kuijer⁹³, A. Kumar¹⁰², J. Kumar⁴⁸, L. Kumar¹⁰⁰, S. Kumar⁴⁸, S. Kundu⁸⁹, P. Kurashvili⁸⁷,
 A. Kurepin⁶³, A.B. Kurepin⁶³, A. Kuryakin¹¹⁰, S. Kushpil⁹⁵, M.J. Kweon⁶¹, Y. Kwon¹⁴⁴, S.L. La Pointe⁴²,
 P. La Rocca²⁸, C. Lagana Fernandes¹²³, Y.S. Lai⁸³, I. Lakomov³⁵, R. Langoy⁴¹, K. Lapidus¹⁴³, C. Lara⁷⁰,
 A. Lardeux^{76,21}, A. Lattuca²⁶, E. Laudi³⁵, R. Lavicka³⁹, R. Lea²⁵, L. Leardini¹⁰⁵, S. Lee¹⁴⁴, F. Lehas⁹³,
 S. Lehner¹¹⁵, J. Lehrbach⁴², R.C. Lemmon⁹⁴, V. Lenti⁵³, E. Leogrande⁶⁴, I. León Monzón¹²², P. Lévai¹⁴²,
 X. Li¹⁴, J. Lien⁴¹, R. Lietava¹¹², B. Lim¹⁹, S. Lindal²¹, V. Lindenstruth⁴², S.W. Lindsay¹²⁸,
 C. Lippmann¹⁰⁸, M.A. Lisa¹⁸, V. Litichevskiy⁴⁶, W.J. Llope¹⁴¹, D.F. Lodato⁶⁴, P.I. Loenne²², V. Loginov⁸⁴,
 C. Loizides⁸³, P. Loncar¹¹⁹, X. Lopez¹³³, E. López Torres⁹, A. Lowe¹⁴², P. Luettig⁷¹, J.R. Luhder⁷²,
 M. Lunardon²⁹, G. Luparello^{60,25}, M. Lupi³⁵, T.H. Lutz¹⁴³, A. Maevskaya⁶³, M. Mager³⁵, S. Mahajan¹⁰²,
 S.M. Mahmood²¹, A. Maire¹³⁵, R.D. Majka¹⁴³, M. Malaev⁹⁷, L. Malinina^{78,iv}, D. Mal'Kevich⁶⁵,
 P. Malzacher¹⁰⁸, A. Mamonov¹¹⁰, V. Manko⁹¹, F. Manso¹³³, V. Manzari⁵³, Y. Mao⁷,
 M. Marchisone^{77,130}, J. Mareš⁶⁷, G.V. Margagliotti²⁵, A. Margotti⁵⁴, J. Margutti⁶⁴, A. Marín¹⁰⁸,
 C. Markert¹²¹, M. Marquard⁷¹, N.A. Martin¹⁰⁸, P. Martinengo³⁵, J.A.L. Martinez⁷⁰, M.I. Martínez²,
 G. Martínez García¹¹⁶, M. Martínez Pedreira³⁵, S. Masciocchi¹⁰⁸, M. Maserà²⁶, A. Masoni⁵⁵,
 E. Masson¹¹⁶, A. Mastroserio⁵³, A.M. Mathis^{106,36}, P.F.T. Matuoka¹²³, A. Matyja¹²⁹, C. Mayer¹²⁰,
 J. Mazer¹²⁹, M. Mazzilli³³, M.A. Mazzoni⁵⁸, F. Meddi²³, Y. Melikyan⁸⁴, A. Menchaca-Rocha⁷⁵,

E. Meninno³⁰, J. Mercado Pérez¹⁰⁵, M. Meres³⁸, S. Mhlanga¹⁰¹, Y. Miake¹³², M.M. Mieskolainen⁴⁶,
 D.L. Mihaylov¹⁰⁶, K. Mikhaylov^{65,78}, J. Milosevic²¹, A. Mischke⁶⁴, A.N. Mishra⁴⁹, D. Miśkowiec¹⁰⁸,
 J. Mitra¹³⁹, C.M. Mitu⁶⁹, N. Mohammadi⁶⁴, B. Mohanty⁸⁹, M. Mohisin Khan^{17,v}, E. Montes¹⁰,
 D.A. Moreira De Godoy⁷², L.A.P. Moreno², S. Moretto²⁹, A. Morreale¹¹⁶, A. Morsch³⁵, V. Muccifora⁵¹,
 E. Mudnic¹¹⁹, D. Mühlheim⁷², S. Muhuri¹³⁹, M. Mukherjee⁴, J.D. Mulligan¹⁴³, M.G. Munhoz¹²³,
 K. Mürning⁴⁵, R.H. Munzer⁷¹, H. Murakami¹³¹, S. Murray⁷⁷, L. Musa³⁵, J. Musinsky⁶⁶, C.J. Myers¹²⁶,
 J.W. Myrcha¹⁴⁰, D. Nag⁴, B. Naik⁴⁸, R. Nair⁸⁷, B.K. Nandi⁴⁸, R. Nania^{54,12}, E. Nappi⁵³, A. Narayan⁴⁸,
 M.U. Naru¹⁵, H. Natal da Luz¹²³, C. Nattrass¹²⁹, S.R. Navarro², K. Nayak⁸⁹, R. Nayak⁴⁸, T.K. Nayak¹³⁹,
 S. Nazarenko¹¹⁰, A. Nedosekin⁶⁵, R.A. Negrao De Oliveira³⁵, L. Nellen⁷³, S.V. Nesbo³⁷, F. Ng¹²⁶,
 M. Nicassio¹⁰⁸, M. Niculescu⁶⁹, J. Niedziela^{140,35}, B.S. Nielsen⁹², S. Nikolaev⁹¹, S. Nikulin⁹¹,
 V. Nikulin⁹⁷, F. Noferini^{12,54}, P. Nomokonov⁷⁸, G. Nooren⁶⁴, J.C.C. Noris², J. Norman¹²⁸, A. Nyanin⁹¹,
 J. Nystrand²², H. Oeschler^{19,105,i}, S. Oh¹⁴³, A. Ohlson^{35,105}, T. Okubo⁴⁷, L. Olah¹⁴², J. Oleniacz¹⁴⁰,
 A.C. Oliveira Da Silva¹²³, M.H. Oliver¹⁴³, J. Onderwaater¹⁰⁸, C. Oppedisano⁵⁹, R. Orava⁴⁶, M. Oravec¹¹⁸,
 A. Ortiz Velasquez⁷³, A. Oskarsson³⁴, J. Otwinowski¹²⁰, K. Oyama⁸⁵, Y. Pachmayer¹⁰⁵, V. Pacik⁹²,
 D. Pagano¹³⁷, P. Pagano³⁰, G. Paic⁷³, P. Palni⁷, J. Pan¹⁴¹, A.K. Pandey⁴⁸, S. Panebianco⁷⁶, V. Papikyan¹,
 G.S. Pappalardo⁵⁶, P. Pareek⁴⁹, J. Park⁶¹, S. Parmar¹⁰⁰, A. Passfeld⁷², S.P. Pathak¹²⁶, R.N. Patra¹³⁹,
 B. Paul⁵⁹, H. Pei⁷, T. Peitzmann⁶⁴, X. Peng⁷, L.G. Pereira⁷⁴, H. Pereira Da Costa⁷⁶, D. Peresunko^{91,84},
 E. Perez Lezama⁷¹, V. Peskov⁷¹, Y. Pestov⁵, V. Petráček³⁹, V. Petrov¹¹⁴, M. Petrovici⁸⁸, C. Petta²⁸,
 R.P. Pezzi⁷⁴, S. Piano⁶⁰, M. Pikna³⁸, P. Pillot¹¹⁶, L.O.D.L. Pimentel⁹², O. Pinazza^{54,35}, L. Pinsky¹²⁶,
 D.B. Piyarathna¹²⁶, M. Płoskoń⁸³, M. Planinic⁹⁹, F. Pliquett⁷¹, J. Pluta¹⁴⁰, S. Pochybova¹⁴²,
 P.L.M. Podesta-Lerma¹²², M.G. Poghosyan⁹⁶, B. Polichtchouk¹¹⁴, N. Poljak⁹⁹, W. Poonsawat¹¹⁷, A. Pop⁸⁸,
 H. Poppenborg⁷², S. Porteboeuf-Houssais¹³³, V. Pozdniakov⁷⁸, S.K. Prasad⁴, R. Preghenella⁵⁴, F. Prino⁵⁹,
 C.A. Pruneau¹⁴¹, I. Pshenichnov⁶³, M. Puccio²⁶, G. Puddu²⁴, P. Pujahari¹⁴¹, V. Punin¹¹⁰, J. Putschke¹⁴¹,
 S. Raha⁴, S. Rajput¹⁰², J. Rak¹²⁷, A. Rakotozafindrabe⁷⁶, L. Ramello³², F. Rami¹³⁵, D.B. Rana¹²⁶,
 R. Raniwala¹⁰³, S. Raniwala¹⁰³, S.S. Räsänen⁴⁶, B.T. Rascanu⁷¹, D. Rathee¹⁰⁰, V. Ratza⁴⁵, I. Ravasenga³¹,
 K.F. Read^{129,96}, K. Redlich^{87,vi}, A. Rehman²², P. Reichelt⁷¹, F. Reidt³⁵, X. Ren⁷, R. Renfordt⁷¹,
 A.R. Reolon⁵¹, A. Reshetin⁶³, K. Reygers¹⁰⁵, V. Riabov⁹⁷, R.A. Ricci⁵², T. Richert³⁴, M. Richter²¹,
 P. Riedler³⁵, W. Riegler³⁵, F. Riggi²⁸, C. Ristea⁶⁹, M. Rodríguez Cahuantzi², K. Røed²¹, E. Rogochaya⁷⁸,
 D. Rohr^{35,42}, D. Röhrich²², P.S. Rokita¹⁴⁰, F. Ronchetti⁵¹, E.D. Rosas⁷³, P. Rosnet¹³³, A. Rossi^{29,57},
 A. Rotondi¹³⁶, F. Roukoutakis⁸⁶, A. Roy⁴⁹, C. Roy¹³⁵, P. Roy¹¹¹, A.J. Rubio Montero¹⁰, O.V. Rueda⁷³,
 R. Rui²⁵, B. Rumyantsev⁷⁸, A. Rustamov⁹⁰, E. Ryabinkin⁹¹, Y. Ryabov⁹⁷, A. Rybicki¹²⁰, S. Saarinen⁴⁶,
 S. Sadhu¹³⁹, S. Sadovsky¹¹⁴, K. Šafařík³⁵, S.K. Saha¹³⁹, B. Sahlmuller⁷¹, B. Sahoo⁴⁸, P. Sahoo⁴⁹,
 R. Sahoo⁴⁹, S. Sahoo⁶⁸, P.K. Sahu⁶⁸, J. Saini¹³⁹, S. Sakai¹³², M.A. Saleh¹⁴¹, J. Salzwedel¹⁸, S. Sambyal¹⁰²,
 V. Samsonov^{97,84}, A. Sandoval⁷⁵, D. Sarkar¹³⁹, N. Sarkar¹³⁹, P. Sarma⁴⁴, M.H.P. Sas⁶⁴, E. Scapparone⁵⁴,
 F. Scarlassara²⁹, B. Schaefer⁹⁶, R.P. Scharenberg¹⁰⁷, H.S. Scheid⁷¹, C. Schiaua⁸⁸, R. Schicker¹⁰⁵,
 C. Schmidt¹⁰⁸, H.R. Schmidt¹⁰⁴, M.O. Schmidt¹⁰⁵, M. Schmidt¹⁰⁴, N.V. Schmidt^{71,96}, J. Schukraft³⁵,
 Y. Schutz^{135,35}, K. Schwarz¹⁰⁸, K. Schweda¹⁰⁸, G. Scioli²⁷, E. Scomparin⁵⁹, M. Šefčík⁴⁰, J.E. Seger⁹⁸,
 Y. Sekiguchi¹³¹, D. Sekihata⁴⁷, I. Selyuzhenkov^{108,84}, K. Senosi⁷⁷, S. Senyukov^{3,35,135}, E. Serradilla^{75,10},
 P. Sett⁴⁸, A. Sevcenco⁶⁹, A. Shabanov⁶³, A. Shabetai¹¹⁶, R. Shahoyan³⁵, W. Shaikh¹¹¹, A. Shangaraev¹¹⁴,
 A. Sharma¹⁰⁰, A. Sharma¹⁰², M. Sharma¹⁰², M. Sharma¹⁰², N. Sharma^{129,100}, A.I. Sheikh¹³⁹,
 K. Shigaki⁴⁷, Q. Shou⁷, K. Shtejer^{26,9}, Y. Sibiriak⁹¹, S. Siddhanta⁵⁵, K.M. Sielewicz³⁵, T. Siemiarczuk⁸⁷,
 S. Silaeva⁹¹, D. Silvermyr³⁴, C. Silvestre⁸², G. Simatovic⁹⁹, G. Simonetti³⁵, R. Singaraju¹³⁹, R. Singh⁸⁹,
 V. Singhal¹³⁹, T. Sinha¹¹¹, B. Sitar³⁸, M. Sitta³², T.B. Skaali²¹, M. Slupecki¹²⁷, N. Smirnov¹⁴³,
 R.J.M. Snellings⁶⁴, T.W. Snellman¹²⁷, J. Song¹⁹, M. Song¹⁴⁴, F. Soramel²⁹, S. Sorensen¹²⁹, F. Sozzi¹⁰⁸,
 E. Spiriti⁵¹, I. Sputowska¹²⁰, B.K. Srivastava¹⁰⁷, J. Stachel¹⁰⁵, I. Stan⁶⁹, P. Stankus⁹⁶, E. Stenlund³⁴,
 D. Stocco¹¹⁶, M.M. Storetvedt³⁷, P. Strmen³⁸, A.A.P. Suaide¹²³, T. Sugitate⁴⁷, C. Suire⁶²,
 M. Suleymanov¹⁵, M. Suljic²⁵, R. Sultanov⁶⁵, M. Šumbera⁹⁵, S. Sumowidagdo⁵⁰, K. Suzuki¹¹⁵,
 S. Swain⁶⁸, A. Szabo³⁸, I. Szarka³⁸, U. Tabassam¹⁵, J. Takahashi¹²⁴, G.J. Tambave²², N. Tanaka¹³²,
 M. Tarhini⁶², M. Tariq¹⁷, M.G. Tarzila⁸⁸, A. Tauro³⁵, G. Tejada Muñoz², A. Telesca³⁵, K. Terasaki¹³¹,
 C. Terrevoli²⁹, B. Teyssier¹³⁴, D. Thakur⁴⁹, S. Thakur¹³⁹, D. Thomas¹²¹, F. Thoresen⁹², R. Tieulent¹³⁴,
 A. Tikhonov⁶³, A.R. Timmins¹²⁶, A. Toia⁷¹, S.R. Torres¹²², S. Tripathy⁴⁹, S. Trogolo²⁶, G. Trombetta³³,
 L. Tropp⁴⁰, V. Trubnikov³, W.H. Trzaska¹²⁷, B.A. Trzeciak⁶⁴, T. Tsuji¹³¹, A. Tumkin¹¹⁰, R. Turrisi⁵⁷,

T.S. Tveter²¹, K. Ullaland²², E.N. Umaka¹²⁶, A. Uras¹³⁴, G.L. Usai²⁴, A. Utrobicic⁹⁹, M. Vala^{118,66}, J. Van Der Maarel⁶⁴, J.W. Van Hoorne³⁵, M. van Leeuwen⁶⁴, T. Vanat⁹⁵, P. Vande Vyvre³⁵, D. Varga¹⁴², A. Vargas², M. Vargyas¹²⁷, R. Varma⁴⁸, M. Vasileiou⁸⁶, A. Vasiliev⁹¹, A. Vauthier⁸², O. Vázquez Doce^{106,36}, V. Vechernin¹³⁸, A.M. Veen⁶⁴, A. Velure²², E. Vercellin²⁶, S. Vergara Limón², R. Vernet⁸, R. Vértesi¹⁴², L. Vickovic¹¹⁹, S. Vigolo⁶⁴, J. Viinikainen¹²⁷, Z. Vilakazi¹³⁰, O. Villalobos Baillie¹¹², A. Villatoro Tello², A. Vinogradov⁹¹, L. Vinogradov¹³⁸, T. Virgili³⁰, V. Vislavicius³⁴, A. Vodopyanov⁷⁸, M.A. Völkl^{105,104}, K. Voloshin⁶⁵, S.A. Voloshin¹⁴¹, G. Volpe³³, B. von Haller³⁵, I. Vorobyev^{106,36}, D. Voscek¹¹⁸, D. Vranic^{35,108}, J. Vrláková⁴⁰, B. Wagner²², H. Wang⁶⁴, M. Wang⁷, D. Watanabe¹³², Y. Watanabe^{131,132}, M. Weber¹¹⁵, S.G. Weber¹⁰⁸, D.F. Weiser¹⁰⁵, S.C. Wenzel³⁵, J.P. Wessels⁷², U. Westerhoff⁷², A.M. Whitehead¹⁰¹, J. Wiechula⁷¹, J. Wikne²¹, G. Wilk⁸⁷, J. Wilkinson^{105,54}, G.A. Willems^{35,72}, M.C.S. Williams⁵⁴, E. Willsher¹¹², B. Windelband¹⁰⁵, W.E. Witt¹²⁹, S. Yalcin⁸¹, K. Yamakawa⁴⁷, P. Yang⁷, S. Yano⁴⁷, Z. Yin⁷, H. Yokoyama^{132,82}, I.-K. Yoo¹⁹, J.H. Yoon⁶¹, V. Yurchenko³, V. Zaccolo⁵⁹, A. Zaman¹⁵, C. Zampolli³⁵, H.J.C. Zanoli¹²³, N. Zardoshti¹¹², A. Zarochentsev¹³⁸, P. Závada⁶⁷, N. Zaviyalov¹¹⁰, H. Zbroszczyk¹⁴⁰, M. Zhalov⁹⁷, H. Zhang^{22,7}, X. Zhang⁷, Y. Zhang⁷, C. Zhang⁶⁴, Z. Zhang^{7,133}, C. Zhao²¹, N. Zhigareva⁶⁵, D. Zhou⁷, Y. Zhou⁹², Z. Zhou²², H. Zhu²², J. Zhu⁷, A. Zichichi^{27,12}, A. Zimmermann¹⁰⁵, M.B. Zimmermann³⁵, G. Zinovjev³, J. Zmeskal¹¹⁵, S. Zou⁷

¹ A.I. Alikhanyan National Science Laboratory (Yerevan Physics Institute) Foundation, Yerevan, Armenia

² Benemérita Universidad Autónoma de Puebla, Puebla, Mexico

³ Bogolyubov Institute for Theoretical Physics, Kiev, Ukraine

⁴ Bose Institute, Department of Physics and Centre for Astroparticle Physics and Space Science (CAPSS), Kolkata, India

⁵ Budker Institute for Nuclear Physics, Novosibirsk, Russia

⁶ California Polytechnic State University, San Luis Obispo, CA, United States

⁷ Central China Normal University, Wuhan, China

⁸ Centre de Calcul de l'IN2P3, Villeurbanne, Lyon, France

⁹ Centro de Aplicaciones Tecnológicas y Desarrollo Nuclear (CEADEN), Havana, Cuba

¹⁰ Centro de Investigaciones Energéticas Medioambientales y Tecnológicas (CIEMAT), Madrid, Spain

¹¹ Centro de Investigación y de Estudios Avanzados (CINVESTAV), Mexico City and Mérida, Mexico

¹² Centro Fermi – Museo Storico della Fisica e Centro Studi e Ricerche "Enrico Fermi", Rome, Italy

¹³ Chicago State University, Chicago, IL, United States

¹⁴ China Institute of Atomic Energy, Beijing, China

¹⁵ COMSATS Institute of Information Technology (CIIT), Islamabad, Pakistan

¹⁶ Departamento de Física de Partículas and IGFAE, Universidad de Santiago de Compostela, Santiago de Compostela, Spain

¹⁷ Department of Physics, Aligarh Muslim University, Aligarh, India

¹⁸ Department of Physics, Ohio State University, Columbus, OH, United States

¹⁹ Department of Physics, Pusan National University, Pusan, Republic of Korea

²⁰ Department of Physics, Sejong University, Seoul, Republic of Korea

²¹ Department of Physics, University of Oslo, Oslo, Norway

²² Department of Physics and Technology, University of Bergen, Bergen, Norway

²³ Dipartimento di Fisica dell'Università 'La Sapienza' and Sezione INFN, Rome, Italy

²⁴ Dipartimento di Fisica dell'Università and Sezione INFN, Cagliari, Italy

²⁵ Dipartimento di Fisica dell'Università and Sezione INFN, Trieste, Italy

²⁶ Dipartimento di Fisica dell'Università and Sezione INFN, Turin, Italy

²⁷ Dipartimento di Fisica e Astronomia dell'Università and Sezione INFN, Bologna, Italy

²⁸ Dipartimento di Fisica e Astronomia dell'Università and Sezione INFN, Catania, Italy

²⁹ Dipartimento di Fisica e Astronomia dell'Università and Sezione INFN, Padova, Italy

³⁰ Dipartimento di Fisica 'E.R. Caianiello' dell'Università and Gruppo Collegato INFN, Salerno, Italy

³¹ Dipartimento DISAT del Politecnico and Sezione INFN, Turin, Italy

³² Dipartimento di Scienze e Innovazione Tecnologica dell'Università del Piemonte Orientale and INFN Sezione di Torino, Alessandria, Italy

³³ Dipartimento Interateneo di Fisica 'M. Merlin' and Sezione INFN, Bari, Italy

³⁴ Division of Experimental High Energy Physics, University of Lund, Lund, Sweden

³⁵ European Organization for Nuclear Research (CERN), Geneva, Switzerland

³⁶ Excellence Cluster Universe, Technische Universität München, Munich, Germany

³⁷ Faculty of Engineering, Bergen University College, Bergen, Norway

³⁸ Faculty of Mathematics, Physics and Informatics, Comenius University, Bratislava, Slovakia

³⁹ Faculty of Nuclear Sciences and Physical Engineering, Czech Technical University in Prague, Prague, Czech Republic

⁴⁰ Faculty of Science, P.J. Šafárik University, Košice, Slovakia

⁴¹ Faculty of Technology, Buskerud and Vestfold University College, Tonsberg, Norway

⁴² Frankfurt Institute for Advanced Studies, Johann Wolfgang Goethe-Universität Frankfurt, Frankfurt, Germany

⁴³ Gangneung-Wonju National University, Gangneung, Republic of Korea

⁴⁴ Gauhati University, Department of Physics, Guwahati, India

⁴⁵ Helmholtz-Institut für Strahlen- und Kernphysik, Rheinische Friedrich-Wilhelms-Universität Bonn, Bonn, Germany

⁴⁶ Helsinki Institute of Physics (HIP), Helsinki, Finland

⁴⁷ Hiroshima University, Hiroshima, Japan

⁴⁸ Indian Institute of Technology Bombay (IIT), Mumbai, India

⁴⁹ Indian Institute of Technology Indore, Indore, India

⁵⁰ Indonesian Institute of Sciences, Jakarta, Indonesia

⁵¹ INFN, Laboratori Nazionali di Frascati, Frascati, Italy

⁵² INFN, Laboratori Nazionali di Legnaro, Legnaro, Italy

⁵³ INFN, Sezione di Bari, Bari, Italy

- 54 INFN, Sezione di Bologna, Bologna, Italy
- 55 INFN, Sezione di Cagliari, Cagliari, Italy
- 56 INFN, Sezione di Catania, Catania, Italy
- 57 INFN, Sezione di Padova, Padova, Italy
- 58 INFN, Sezione di Roma, Rome, Italy
- 59 INFN, Sezione di Torino, Turin, Italy
- 60 INFN, Sezione di Trieste, Trieste, Italy
- 61 Inha University, Incheon, Republic of Korea
- 62 Institut de Physique Nucléaire d'Orsay (IPNO), Université Paris-Sud, CNRS-IN2P3, Orsay, France
- 63 Institute for Nuclear Research, Academy of Sciences, Moscow, Russia
- 64 Institute for Subatomic Physics of Utrecht University, Utrecht, Netherlands
- 65 Institute for Theoretical and Experimental Physics, Moscow, Russia
- 66 Institute of Experimental Physics, Slovak Academy of Sciences, Košice, Slovakia
- 67 Institute of Physics, Academy of Sciences of the Czech Republic, Prague, Czech Republic
- 68 Institute of Physics, Bhubaneswar, India
- 69 Institute of Space Science (ISS), Bucharest, Romania
- 70 Institut für Informatik, Johann Wolfgang Goethe-Universität Frankfurt, Frankfurt, Germany
- 71 Institut für Kernphysik, Johann Wolfgang Goethe-Universität Frankfurt, Frankfurt, Germany
- 72 Institut für Kernphysik, Westfälische Wilhelms-Universität Münster, Münster, Germany
- 73 Instituto de Ciencias Nucleares, Universidad Nacional Autónoma de México, Mexico City, Mexico
- 74 Instituto de Física, Universidade Federal do Rio Grande do Sul (UFRGS), Porto Alegre, Brazil
- 75 Instituto de Física, Universidad Nacional Autónoma de México, Mexico City, Mexico
- 76 IRFU, CEA, Université Paris-Saclay, Saclay, France
- 77 iThemba LABS, National Research Foundation, Somerset West, South Africa
- 78 Joint Institute for Nuclear Research (JINR), Dubna, Russia
- 79 Konkuk University, Seoul, Republic of Korea
- 80 Korea Institute of Science and Technology Information, Daejeon, Republic of Korea
- 81 KTO Karatay University, Konya, Turkey
- 82 Laboratoire de Physique Subatomique et de Cosmologie, Université Grenoble-Alpes, CNRS-IN2P3, Grenoble, France
- 83 Lawrence Berkeley National Laboratory, Berkeley, CA, United States
- 84 Moscow Engineering Physics Institute, Moscow, Russia
- 85 Nagasaki Institute of Applied Science, Nagasaki, Japan
- 86 National and Kapodistrian University of Athens, Physics Department, Athens, Greece
- 87 National Centre for Nuclear Studies, Warsaw, Poland
- 88 National Institute for Physics and Nuclear Engineering, Bucharest, Romania
- 89 National Institute of Science Education and Research, HBNI, Jatni, India
- 90 National Nuclear Research Center, Baku, Azerbaijan
- 91 National Research Centre Kurchatov Institute, Moscow, Russia
- 92 Niels Bohr Institute, University of Copenhagen, Copenhagen, Denmark
- 93 Nikhef, Nationaal instituut voor subatomaire fysica, Amsterdam, Netherlands
- 94 Nuclear Physics Group, STFC Daresbury Laboratory, Daresbury, United Kingdom
- 95 Nuclear Physics Institute, Academy of Sciences of the Czech Republic, Řež u Prahy, Czech Republic
- 96 Oak Ridge National Laboratory, Oak Ridge, TN, United States
- 97 Petersburg Nuclear Physics Institute, Gatchina, Russia
- 98 Physics Department, Creighton University, Omaha, NE, United States
- 99 Physics Department, Faculty of Science, University of Zagreb, Zagreb, Croatia
- 100 Physics Department, Panjab University, Chandigarh, India
- 101 Physics Department, University of Cape Town, Cape Town, South Africa
- 102 Physics Department, University of Jammu, Jammu, India
- 103 Physics Department, University of Rajasthan, Jaipur, India
- 104 Physikalisches Institut, Eberhard Karls Universität Tübingen, Tübingen, Germany
- 105 Physikalisches Institut, Ruprecht-Karls-Universität Heidelberg, Heidelberg, Germany
- 106 Physik Department, Technische Universität München, Munich, Germany
- 107 Purdue University, West Lafayette, IN, United States
- 108 Research Division and ExtreMe Matter Institute EMMI, GSI Helmholtzzentrum für Schwerionenforschung GmbH, Darmstadt, Germany
- 109 Rudjer Bošković Institute, Zagreb, Croatia
- 110 Russian Federal Nuclear Center (VNIIEF), Sarov, Russia
- 111 Saha Institute of Nuclear Physics, Kolkata, India
- 112 School of Physics and Astronomy, University of Birmingham, Birmingham, United Kingdom
- 113 Sección Física, Departamento de Ciencias, Pontificia Universidad Católica del Perú, Lima, Peru
- 114 SSC IHEP of NRC Kurchatov institute, Protvino, Russia
- 115 Stefan Meyer Institut für Subatomare Physik (SMI), Vienna, Austria
- 116 SUBATECH, IMT Atlantique, Université de Nantes, CNRS-IN2P3, Nantes, France
- 117 Suranaree University of Technology, Nakhon Ratchasima, Thailand
- 118 Technical University of Košice, Košice, Slovakia
- 119 Technical University of Split FESB, Split, Croatia
- 120 The Henryk Niewodniczanski Institute of Nuclear Physics, Polish Academy of Sciences, Cracow, Poland
- 121 The University of Texas at Austin, Physics Department, Austin, TX, United States
- 122 Universidad Autónoma de Sinaloa, Culiacán, Mexico
- 123 Universidade de São Paulo (USP), São Paulo, Brazil
- 124 Universidade Estadual de Campinas (UNICAMP), Campinas, Brazil
- 125 Universidade Federal do ABC, Santo Andre, Brazil
- 126 University of Houston, Houston, TX, United States
- 127 University of Jyväskylä, Jyväskylä, Finland
- 128 University of Liverpool, Liverpool, United Kingdom
- 129 University of Tennessee, Knoxville, TN, United States
- 130 University of the Witwatersrand, Johannesburg, South Africa
- 131 University of Tokyo, Tokyo, Japan
- 132 University of Tsukuba, Tsukuba, Japan

- ¹³³ *Université Clermont Auvergne, CNRS/IN2P3, LPC, Clermont-Ferrand, France*
¹³⁴ *Université de Lyon, Université Lyon 1, CNRS/IN2P3, IPN-Lyon, Villeurbanne, Lyon, France*
¹³⁵ *Université de Strasbourg, CNRS, IPHC UMR 7178, F-67000 Strasbourg, France*
¹³⁶ *Università degli Studi di Pavia, Pavia, Italy*
¹³⁷ *Università di Brescia, Brescia, Italy*
¹³⁸ *V. Fock Institute for Physics, St. Petersburg State University, St. Petersburg, Russia*
¹³⁹ *Variable Energy Cyclotron Centre, Kolkata, India*
¹⁴⁰ *Warsaw University of Technology, Warsaw, Poland*
¹⁴¹ *Wayne State University, Detroit, MI, United States*
¹⁴² *Wigner Research Centre for Physics, Hungarian Academy of Sciences, Budapest, Hungary*
¹⁴³ *Yale University, New Haven, CT, United States*
¹⁴⁴ *Yonsei University, Seoul, Republic of Korea*
¹⁴⁵ *Zentrum für Technologietransfer und Telekommunikation (ZTT), Fachhochschule Worms, Worms, Germany*

ⁱ Deceased

ⁱⁱ Dipartimento DET del Politecnico di Torino, Turin, Italy.

ⁱⁱⁱ Georgia State University, Atlanta, Georgia, United States.

^{iv} M.V. Lomonosov Moscow State University, D.V. Skobeltsyn Institute of Nuclear Physics, Moscow, Russia.

^v Department of Applied Physics, Aligarh Muslim University, Aligarh, India.

^{vi} Institute of Theoretical Physics, University of Wrocław, Poland.